9/30/03 9:38 AM
LBNL-53814

FRACTURE AND FATIGUE RESISTANCE OF Mo-Si-B ALLOYS FOR ULTRAHIGH-TEMPERATURE STRUCTURAL APPLICATIONS

***J. J. Kruzic*[1], *J. H. Schneibel*[2], *and R. O. Ritchie*[1]**

[1]Materials Sciences Division, Lawrence Berkeley National Laboratory, and
Department of Materials Science and Engineering,
University of California, Berkeley, CA 94720, USA

[2]Oak Ridge National Laboratory, Metals and Ceramics Division, Oak Ridge, TN 37831

submitted to
Scripta Materialia

Sept. 2003

Work supported by the U.S. Department of Energy: (i) by the Office of Science, Office of Basic Energy Sciences, Division of Materials Sciences and Engineering under Contract No. DE-AC03-76SF00098 with the Lawrence Berkeley National Laboratory (for JJK and ROR), and (ii) by the Office of Fossil Energy, Advanced Research Materials Program under Contract No. DE-AC05-00OR22725 with Oak Ridge National Laboratory managed by UT-Battelle, LLC (for JHS).

Fracture and Fatigue Resistance of Mo-Si-B Alloys for Ultrahigh-Temperature Structural Applications

J. J. Kruzic[1], J. H. Schneibel[2], and R. O. Ritchie[1*]

[1]Materials Sciences Division, Lawrence Berkeley National Laboratory, and Department of Materials Science and Engineering, University of California, Berkeley, California 94720

[2]Oak Ridge National Laboratory, Metals and Ceramics Division, Oak Ridge, Tennessee 37831

Abstract

Fracture and fatigue-crack growth properties are examined for a series of Mo-Mo_3Si-Mo_5SiB_2 containing alloys, which utilize a continuous α-Mo matrix to achieve unprecedented room-temperature fracture resistance (>20 MPa√m). Mechanistically, these properties are explained in terms of toughening by crack trapping and crack bridging by the more ductile α-Mo phase.

Keywords: Fracture, Fatigue, Toughness, Molybdenum, Silicides

1. Introduction

For applications such as aircraft engines, spacecraft and power generation, future advancements are limited by the availability of higher temperature structural materials. For example, single-crystal nickel-based superalloys have essentially reached their technological limit and are unsuitable for structural use above ~1100°C [1]. High melting-point (>2000°C) materials, based on refractory metals such as molybdenum, represent a higher-temperature alternative but suffer from oxidation and creep problems. In this regard, molybdenum silicides and borosilicides have shown promise in improving the oxidation and creep resistance [2-4], leading to the development of two specific Mo-Si-B alloy systems by Akinc *et al* [2-5] and Berczik *et al* [6,7]; however, the silicide compounds alone are quite brittle and provide little fracture resistance for most structural applications without significant additional toughening. In previous reports [8,9], we have described alloys containing (α-) molybdenum particles surrounded by the hard but brittle

* Corresponding author: Tel: (510) 486-5798; Fax: (510) 486-4881
E-mail address: RORitchie@lbl.gov (R. O. Ritchie)

Mo_3Si and Mo_5SiB_2 (T2) intermetallic phases, which display definitive, but still small, improvements in toughness relative to monolithic silicides. Clearly, the key to achieving high fracture resistance in these materials is in making more effective use of the relatively ductile molybdenum phase, not unlike nickel-base (γ/γ') superalloys, where high fracture toughnesses are obtained with a similarly high fraction of intermetallic (γ') precipitates.

One promising approach is to design Mo-Si-B alloys where the intermetallic phases are completely surrounded by a continuous α-Mo matrix; higher toughness would be expected since incipient cracks would be forced to interact with the locally tougher α-Mo. In this regard, a novel powder processing route has recently been developed to enable the production of such alloys [10]. Accordingly, the objective of the present paper is to present a first investigation into the fracture and fatigue properties of three Mo-20Si-10B at% alloys with continuous α-Mo phase, and to provide an initial description of the micromechanisms responsible for the enhanced toughening.

2. Materials and Procedures

Ground powders of composition Mo-20Si-10B at%, were vacuum annealed to remove silicon from the surface and leave an α-Mo coating on each particle. These surface-modified powders were then hot isostatically pressed in evacuated Nb cans for 4 hr at 1600°C at a pressure of 200 MPa. Three alloys were produced differing in volume fraction of the α-Mo matrix and coarseness of the intermetallic particles. These alloys contained Mo_3Si (cubic A15 structure) and Mo_5SiB_2 or T2 (tetragonal $D8_1$ structure) intermetallic phases within a continuous α-Mo matrix; alloys designated as "fine" and "medium" had 34 vol% α-Mo phase with initial powder sizes of ≤45, 45-90 μm, respectively, while the "coarse" alloy had 49 vol% α-Mo phase and an initial powder size of 90-180 μm (Fig. 1). Tensile tests (strain rate ~3.3×10^{-3} s^{-1}) on the "coarse" alloy revealed brittle failure at room temperature with a strength of 140 MPa, while at 1200°C (*in vacuo*) yield and tensile strengths of 336 and 354 MPa, respectively, were measured with 1.8% elongation.

Resistance-curve (R-curve) fracture toughness experiments were performed on fatigue pre-cracked, disk-shaped, compact-tension DC(T) specimens (width, $W \approx 14$ mm;

thickness, $B \approx 3$mm) in general accordance with ASTM Standard E561. By cyclically loading half-chevron notched specimens, fatigue pre-cracks were introduced and propagated beyond the half-chevron notch region, typically 300 – 600 μm in length. Samples were than loaded monotonically in displacement control at a rate of ~1 μm/min. until the onset of cracking. For room temperature testing, periodic unloads of 10-20% of the peak load were performed to measure the unloading back-face strain compliance, which was used to determine the crack length [11]. Elevated temperature tests (1300°C) were conducted in a gettered argon environment using (direct-current) electrical potential-drop techniques to monitor crack length [12]. In specific instances, testing was paused to observe crack profiles by optical and scanning electron microscopy.

Cyclic fatigue-crack growth testing (25 Hz, sinusoidal waveform) was also performed at 25° and 1300°C in identical respective environments in general accordance with ASTM Standard E647 using computer-controlled servo-hydraulic testing machines at a load ratio (ratio of minimum to maximum loads) of $R = 0.1$. Fatigue-crack growth rates, da/dN, were determined as a function of the stress-intensity range, ΔK, using continuous load-shedding to maintain a normalized ΔK-gradient ($=1/\Delta K[d\Delta K/da]$) of ± 0.08 mm^{-1}. ΔK_{TH} fatigue thresholds, operationally defined as the ΔK corresponding to a minimum growth rate of 10^{-10}–10^{-11} m/cycle, were approached under decreasing ΔK conditions. In all experiments, errors in crack length measurements due to crack bridging (which can affect both compliance and potential-drop measurements) were periodically evaluated by direct optical measurements of the crack size; readings were corrected by assuming that the error accumulated linearly with crack extension.

3. Results

(1) Fracture toughness

Fracture toughness R-curves for the three Mo-Mo_3Si-T2 alloys are shown in Fig. 2; it is apparent that all materials exhibit rising fracture toughness with crack extension. This effect is most dramatic for the "coarse" alloy, which had a peak room-temperature toughness of 21 MPa√m, i.e., up to seven times higher than that of monolithic molybdenum silicides (e.g., $MoSi_2$, Mo_3Si), which have toughness values of 3 to 4

MPa√m [13,14]. Additionally, the toughness of the current alloys is far superior to those previously reported with a discontinuous α-Mo phase; these latter materials displayed very little R-curve behavior with much lower peak toughness ranging from 4 to 7.5 MPa√m [8,9], i.e., they showed only marginal improvements in toughness over monolithic silicides. Additionally, the fracture toughness appeared to improve at higher temperatures; specifically the "medium" alloy displayed a 50% rise in peak toughness from 10 to 15 MPa√m on increasing the temperature from 25° to 1300°C.

(2) Fatigue-crack growth

Room temperature and 1300°C fatigue-crack growth results for all three alloys are shown in Fig. 3. It is apparent from Fig. 3 that crack-growth rates at 25°C have a high dependence on ΔK, which is characteristic of brittle materials. Indeed, when considered in terms of a standard Paris power law, $da/dN \propto \Delta K^m$, the Paris law exponents, m, are, respectively, 125, 87, and 78 for the "fine", "medium", and "coarse" microstructures. At 1300°C, although the "medium" alloy demonstrated a similarly high ΔK dependence, there was a marked change in the behavior of the "coarse" alloy, which displayed more than an order of magnitude decrease in the Paris law exponent to $m \approx 4$. This value of m is more like that of ductile materials, where exponents in conventional metals typically range from 2 to 4.

Fatigue thresholds values of $\Delta K_{TH} \approx 6$, 6.5, and 9.5 MPa√m were measured at 25°C for the "fine", "medium", and "coarse" microstructures, respectively (Fig. 3). At 1300°C, due to the difficulty of experiments and limited number of samples, data was not collected near the operationally defined fatigue threshold; however, based on extrapolation of the data, the threshold for the "medium" microstructure was found to be similar to that at 25°C, whereas the "coarse" microstructure showed a decrease in ΔK_{TH} with increasing temperature to 1300°C.

4. Discussion

(1) Toughening Mechanisms

In order to identify the salient toughening mechanisms responsible for the rising R-curve behavior, tests were periodically interrupted to observe the crack trajectories with optical and scanning electron microscopy. Such examinations revealed a combination of intrinsic and extrinsic toughening mechanisms, most importantly crack trapping and crack bridging, as shown in Fig. 4. While intrinsic toughening mechanisms act ahead of the crack tip and serve to raise the inherent toughness, or crack-initiation point on the R-curve, extrinsic toughening mechanisms generally act behind the crack tip and "shield" the crack from the applied driving force, thereby contributing to rising (crack-growth) toughness with crack extension [15]. In the present case, the intrinsic toughening appears to derive primarily from crack trapping, whereby the crack becomes locally impeded at the more "ductile" α-Mo phase while propagating through the microstructure. Because the trapped crack front preferentially samples the more "ductile" α-Mo phase, the driving force needed to initiate crack advance is higher relative to the unreinforced Mo_3Si and T2 phases. Crack trapping is observed directly in Fig. 4a where the crack tip is seen to arrest at the α-Mo phase. By utilizing a *continuous* α-Mo matrix, crack trapping becomes a more potent toughening mechanism because the crack cannot bypass the α-Mo phase. As a result, the initiation toughness of these alloys ranges from 7.5 to 12 MPa√m, values up to four times higher than for unreinforced molybdenum silicides [13,14].

With respect to the crack-growth toughness, evidence of crack bridging in the wake is also apparent in Fig. 4. Such bridges serve to resist the opening of the crack and are predominantly composed of the α-Mo phase, although some intermetallic bridges were observed. Based on crack-profile observations, bridge formation appears to be a result of cracks renucleating in the more brittle Mo_3Si and T2 phases ahead of the relatively ductile α-Mo regions, i.e., as the crack extends, crack trapping leads to crack bridging (Fig. 4b). Such a process yields regions of α-Mo that bridge the crack wake and sustain load that would otherwise contribute to crack growth. Accordingly, bridging acts to lower the near-tip stress intensity, K_{tip}, relative to the applied stress intensity, K_{app}, by an amount referred to as the bridging stress intensity, K_{br}, i.e., $K_{tip} = K_{app} - K_{br}$. Because bridging is active in the crack wake, it only serves as a toughening mechanism after some

crack extension (i.e., $K_{br} = K_{br}(\Delta a)$), resulting in rising fracture resistance with crack growth. As with crack trapping, the *continuous* α-Mo phase is crucial for the effectiveness of this mechanism because it implies that the crack must interact with the α-Mo phase, i.e., again the crack cannot avoid the α-Mo regions. Toughening from crack bridging gives these materials significantly enhanced damage tolerance, which is important for many structural applications. Engine components, such as turbine blades for example, are subject to phenomena such as foreign-object damage in which case rising R-curve behavior becomes an important property as cracks introduced by the impact events will often be arrested simply by propagating a short distance.

While high-temperature structural materials must have a balance between ambient and elevated temperature strength and fracture resistance, most of the functional life of the component is expected to be at the service (elevated) temperature. In this regard, the increase in fracture resistance exhibited by the "medium" alloy at 1300°C, consistent with other Mo-Si-B alloys [8,9], is a highly desirable property. Observations of crack profiles (Fig. 4) revealed no change in the toughening mechanisms between 25° and 1300°C, implying that the increase in toughness can be associated with the improved ductility of the α-Mo at the higher temperatures. Unalloyed Mo is typically reported to undergo a "brittle-to-ductile" transition between 1000 and 1100°C [16], although this temperature can be significantly lower at slow strain rates. Accordingly, the resulting increases in α-Mo ductility allow for improved effectiveness of both the crack trapping and bridging mechanisms at 1300°C. Indeed, the increased potency of crack trapping is evidenced by the rise in initiation toughness from 7.5 to 12 MPa√m, while the enhanced rising R-curve behavior implies an increased effectiveness of the bridging. Moreover, direct observations of cracking that occurred at 1300°C show significant crack blunting (Fig. 4b) at the trapping α-Mo phase which can be related to the higher measured crack-initiation toughness values; such blunting is not observed at room temperature. Additionally, bridges that formed at 1300°C displayed improved ductility over those formed at low temperatures (Fig. 4c). Higher ductility allows for bridges to deform and remain intact farther behind the crack tip instead of failing prematurely; this leads to larger bridging zones and higher peak toughness values.

(2) Fatigue-Crack Growth

The high Paris law exponents measured for the Mo-Si-B alloys indicate that they show little susceptibility to fatigue damage at room temperature. Additionally, due to this high dependence of growth rates on the stress-intensity range, it is apparent that if cracks do begin to propagate under cyclic loading conditions, they will quickly lead to failure unless they are growing into a diminishing stress field. Accordingly, the fatigue threshold, below which cracks are presumed to be dormant, should be considered as an important parameter characterizing fatigue behavior at low temperatures in these alloys. In this regard, the ΔK_{TH} fatigue thresholds in the Mo-Si-B alloys are a high proportion of the fracture toughness; specifically, the maximum stress intensity at the threshold, $K_{max,TH}$, is ~90% of the initiation toughness for all three microstructures, representing behavior typical of brittle materials.

The paths of the fatigue cracks looked similar to that observed for the fracture specimens, with bridges readily observed spanning the crack wake (Fig. 5a). Upon further propagation of the fatigue crack, these bridges were observed to fail in the wake (Fig. 5b), while new bridges formed near the crack tip. For the fatigue data shown in Fig. 3, a steady-state condition was thought to have been achieved, whereby bridges were created and exhausted at an equal rate, and a bridging zone of roughly constant size was carried along behind the crack tip. This process is similar to the extrinsic fatigue mechanism observed in bridging ceramics [17,18], where fatigue-crack growth is promoted by the failure of bridges in the crack wake, which in turn causes a decrease in K_{br} and a corresponding increase in K_{tip}, leading to crack advance. It is believed that this process is the primary cyclic loading-induced mechanism involved in the fatigue-crack propagation of the present Mo-Si-B alloys at room temperature.

In contrast to ceramics though, the present alloys contain a comparatively "ductile" phase (α-Mo), which should allow for intrinsic mechanisms to additionally contribute to crack advance, i.e., by alternating blunting and resharpening of the crack tip, as in metals. As noted above, at room temperature where the Paris law exponents are so high, the extrinsic mechanism for crack advance (i.e., bridging degradation) dominates; however,

for the "coarse" microstructure at 1300°C, the order of magnitude decrease in Paris law exponent clearly implies more "metal-like" fatigue behavior.

5. Conclusions

Based on an experimental investigation into the ambient to high temperature fracture toughness and fatigue-crack propagation behavior of three Mo-Si-B alloys, containing Mo_3Si and Mo_5SiB_2 intermetallic phases dispersed within a continuous α-Mo matrix, the following conclusions may be made:

1. All three alloys had far superior fracture toughness properties (including rising R-curve behavior) compared to unreinforced molybdenum silicides; moreover, they were significantly tougher than previously reported Mo-Si-B alloys with discrete α-Mo particles. Specifically, at 25°C, the crack-initiation and peak toughness values were 7.5 – 12 and 9 – 21 MPa√m, respectively, with the highest toughnesses achieved with coarse intermetallic particles and higher volume fractions of α-Mo phase.
2. The high toughness of these alloys was attributed to a combination of crack trapping at the α-Mo phase, which raised the initiation toughness, and crack bridging in the crack wake, which contributed to the rising R-curve behaviour. Both mechanisms were promoted by the presence of the continuous α-Mo matrix phase.
3. Based on limited experiments, the fracture resistance appeared to further increase at 1300°C as a result of improved α-Mo ductility; specifically, the "medium" microstructure demonstrated a ~50% increase in both the crack-initiation and peak toughness values at 1300°C compared to room temperature.
4. Although these alloys were not particularly susceptible to fatigue damage at room temperature, fatigue-crack growth was observed to occur via a mechanism of cyclic loading-induced degradation of crack bridging in the crack wake. This extrinsic mechanism resulted in a marked sensitivity of fatigue-crack growth rates to the stress intensity, with Paris law exponents ranging from 80 to 125. ΔK_{TH} fatigue thresholds ranged from 6 to 9.5 MPa√m, with the maximum stress intensity ~90% of the crack-initiation toughness for all alloys.

5. At 1300°C, the "coarse" microstructure demonstrated a change in fatigue behavior marked by an order of magnitude decrease in the Paris law exponent. This shift to more "metal-like" behavior was attributed to the high α-Mo content and its increased ductility at elevated temperatures, which suggested a more intrinsic fatigue mechanism of alternating blunting and resharpening at the crack tip.

Acknowledgements

Work supported by the U.S. Department of Energy (i) by the Office of Science, Office of Basic Energy Sciences, Division of Materials Sciences and Engineering under Contract No. DE-AC03-76SF00098 with the Lawrence Berkeley National Laboratory (for JJK and ROR) and (ii) by the Office of Fossil Energy, Advanced Research Materials Program under Contract No. DE-AC05-00OR22725 with Oak Ridge National Laboratory managed by UT-Battelle, LLC (for JHS).

References

[1] Donachie MJ. Superalloys: A Technical Guide. American Society for Metals, 2002. p. 439.
[2] Meyer MK, Kramer MJ, Akinc M. Intermetallics 1996;4:273.
[3] Akinc M, Meyer MK, Kramer MJ, Thom AJ, Heubsch JJ, Cook B. Mater. Sci. Eng. 1999;A261:16.
[4] Meyer MK, Akinc M. J. Am. Ceram. Soc. 1996;79:2763.
[5] Meyer MK, Thom AJ, Akinc M. Intermetallics 1999;7:153.
[6] Berczik DM. Method for enhancing the oxidation resistance of a molybdenum alloy, and a method of making a molybdenum alloy. United States Patent 5,595,616, 1997.
[7] Berczik DM. Oxidation resistant molybdenum alloys. United States Patent 5,693,156, 1997.
[8] Choe H, Chen D, Schneibel JH, Ritchie RO. Intermetallics 2001;9:319.
[9] Choe H, Schneibel JH, Ritchie RO. Metall. Mater. Trans. 2003;34A:25.
[10] Schneibel JH, Kramer MJ, Easton DS. Scripta Mater. 2002;46:217.
[11] Gilbert CJ, McNaney JM, Dauskardt RH, Ritchie RO. J. Test. Eval. 1994;22:117.
[12] Chen D, Gilbert CJ, Ritchie RO. J. Test. Eval. 2000;28:236.
[13] Venkateswara Rao KT, Soboyejo WO, Ritchie RO. Metall. Trans. 1992;23A:2249.
[14] Rosales I, Schneibel JH. Intermetallics 2000;8:885.
[15] Ritchie RO. Int. J. Fract. 1999;100:55.
[16] Johnson WA. Molybdenum. *Metals Handbook Volume 2 Properties and Selection: Nonferrous Alloys and Special-Purpose Materials* ASM International 1990. p. 574.
[17] Lathabai S, Rödel J, Lawn B. J. Am. Ceram. Soc. 1991;74:1348.
[18] Gilbert CJ, Petrany RN, Ritchie RO, Dauskardt RH, Steinbrech RW. J. Mater. Sci. 1995;30:643.

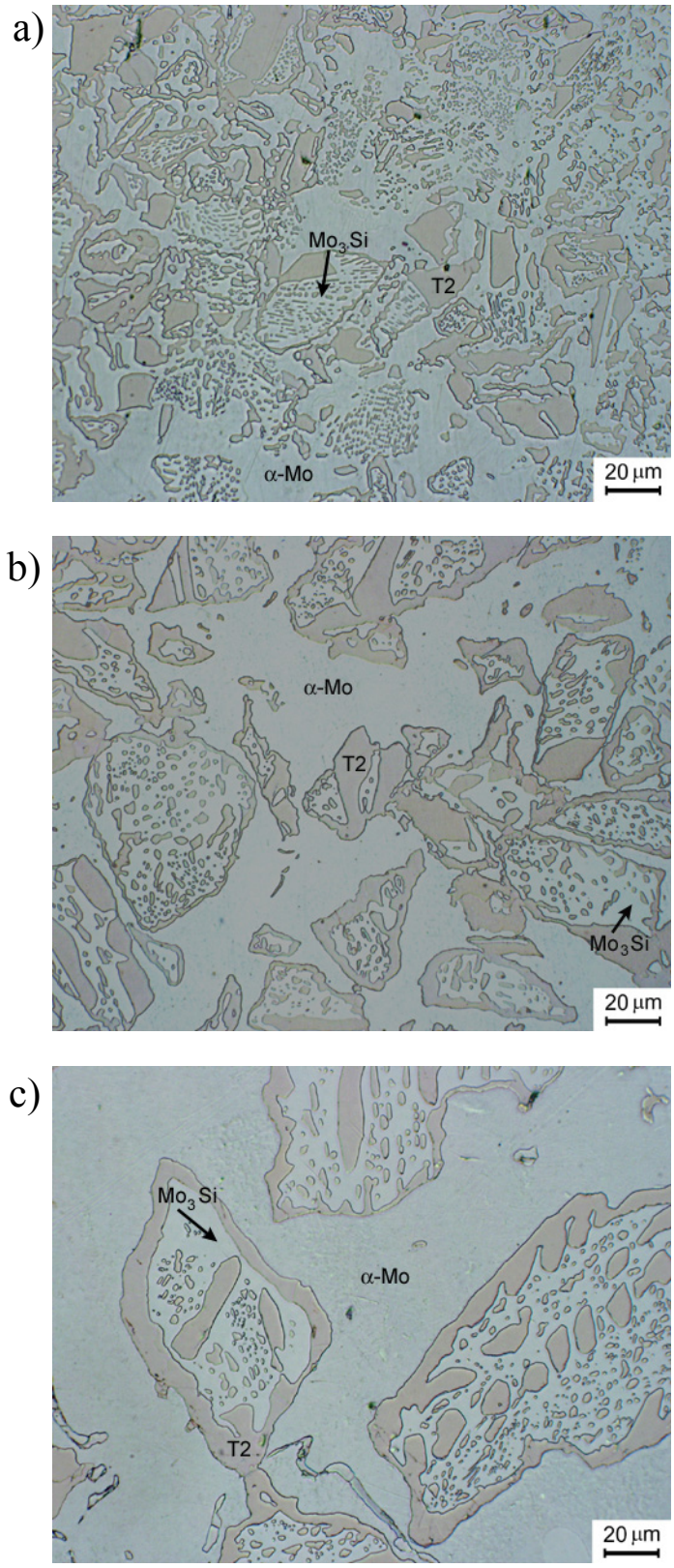

Figure 1: Optical micrographs of the (a) "fine", (b) "medium", and (c) "coarse" alloys, showing a continuous α-Mo matrix with Mo_3Si and T2 (etched in Murakami's reagent).

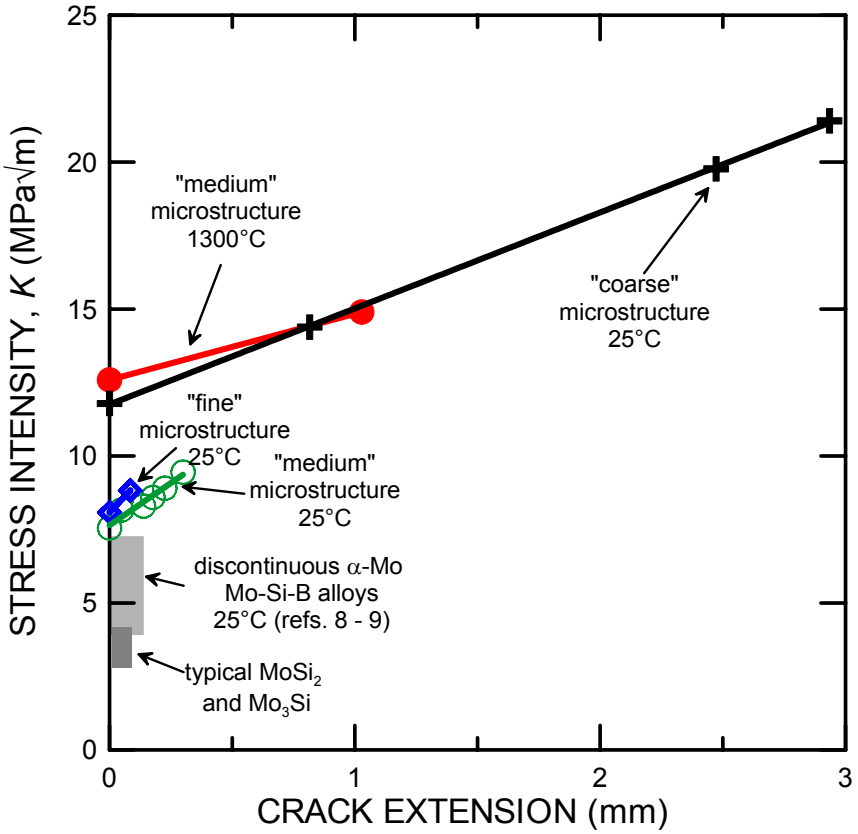

Figure 2: R-curves showing the fracture resistance and fracture toughness of the continuous α-Mo matrix Mo-Si-B alloys. Additionally shown are reported values for unreinforced molybdenum silicides [13,14] and previously reported Mo-Si-B alloys with a discontinuous α-Mo phase [8,9].

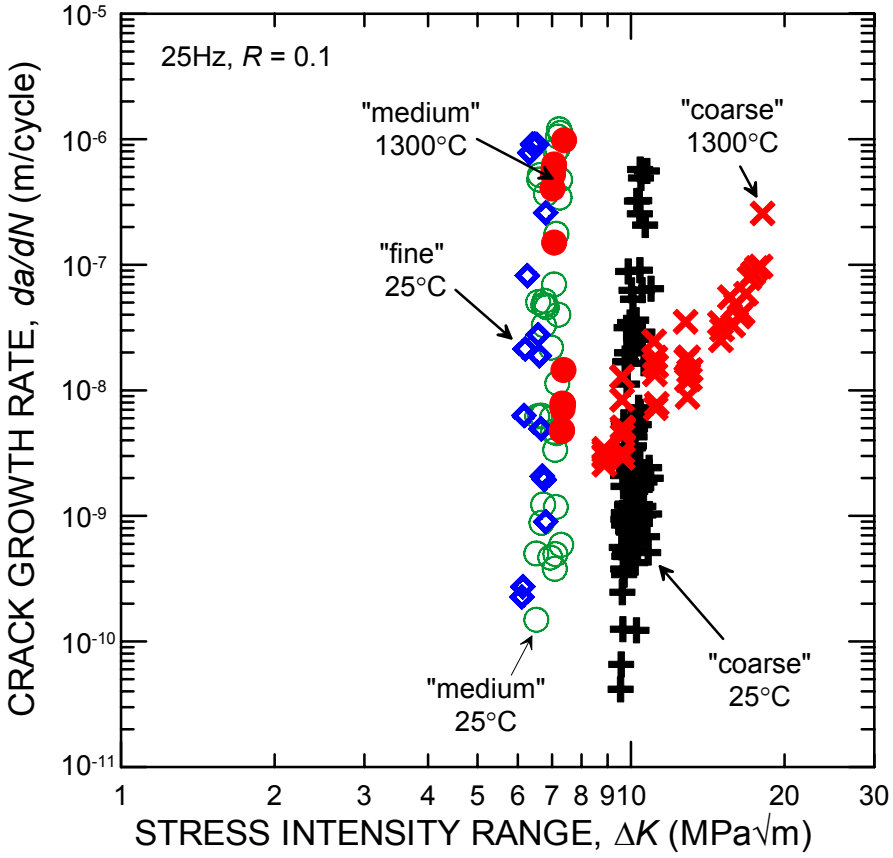

Figure 3: Variation in fatigue-crack growth rates, *da/dN*, as a function of the stress-intensity range, ΔK, for the continuous α-Mo matrix Mo-Si-B alloys at 25°C and 1300°C.

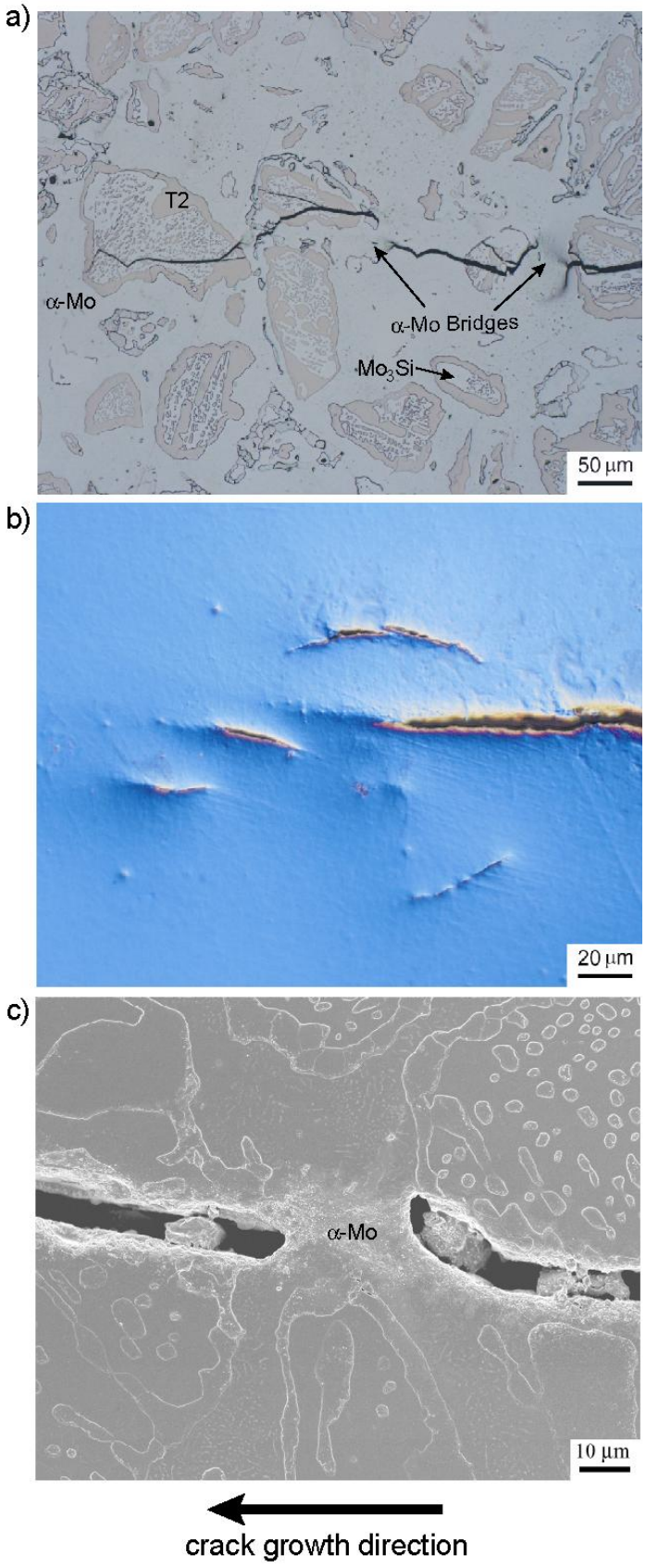
a)
T2
α-Mo
α-Mo Bridges
Mo3Si
50 μm
b)
20 μm
c)
α-Mo
10 μm
crack growth direction

Figure 4: a) Crack trapping and bridging at the α-Mo phase in the "coarse" Mo-Si-B alloy. Note how the crack locally arrests at the α-Mo phase, leaving α-Mo bridges in the crack wake. b) The crack tip in the "medium" alloy after R-curve testing at 1300°C, demonstrating crack blunting at the α-Mo phase, together with the formation of uncracked-ligament bridges near the crack tip. c) Micrograph showing one such "ductile" bridge of an intact α-Mo region, located ~200 μm behind the crack tip, in the "medium" alloy, again fractured at 1300°C. In a) and c), the microstructure was etched with Murakami's reagent.

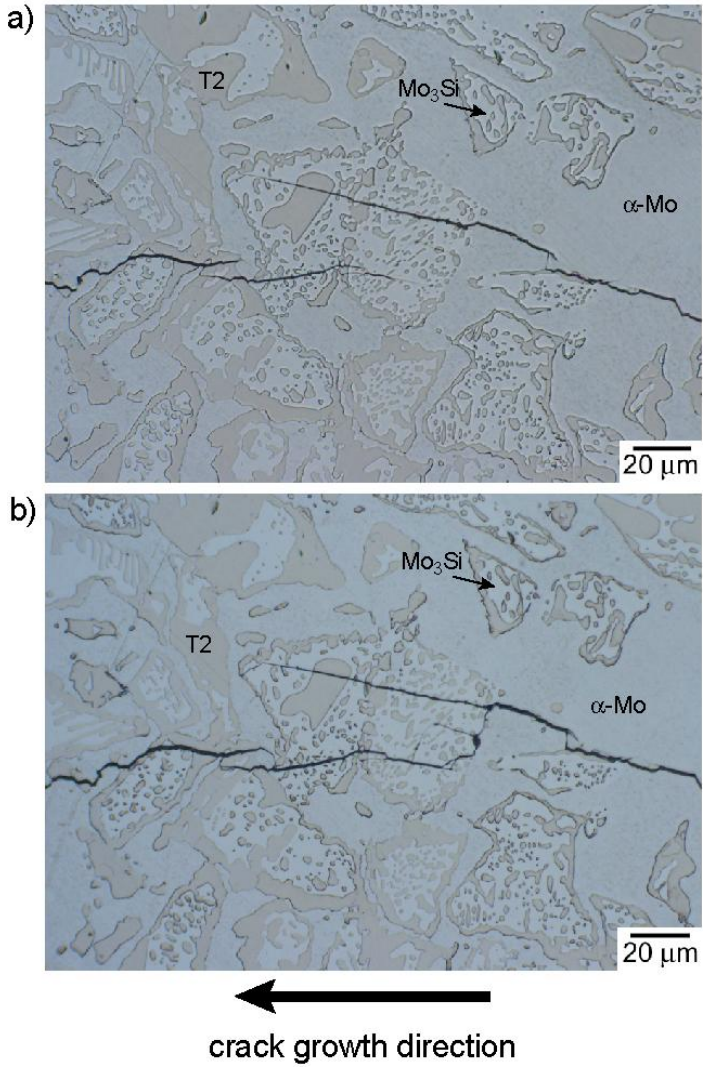

Figure 5: a) Micrograph showing crack bridging ~400 μm behind the crack tip in the "medium" Mo-Si-B microstructure during fatigue-crack growth. b) The same region after the crack tip has extended an additional 800 μm, where the degradation of the bridging can be seen. The microstructure was etched with Murakami's reagent.